# Direct Mesh-Based Model Order Reduction of PEEC Model for Quasi-Static Circuit Problems

Yuhang Dou, *Student Member, IEEE*, and Ke-Li Wu, *Fellow, IEEE*

***Abstract*— In this paper, a new concept of matrix-inversion-less derived physically expressive circuit method of model order reduction for large-scale high-speed/microwave circuit problems is proposed. It is the first model that is derived based on the mesh information of partial element equivalent circuit modeling. This new proposed method absorbs insignificant nodes and parallel branches while retaining the physical meaning of all the inductive and capacitive elements. This method does not involve any matrix inversions or decompositions and its computational overhead is dominated by outer products that can be simply accelerated by the massive GPU acceleration technique. The resultant order-reduced circuit is very useful for not only speeding up the analysis of a large-scale high-speed/microwave circuit but also interpreting the physical insight of the circuit layout from the circuit domain point of view. Three numerical examples are given, demonstrating the versatility, scalability, accuracy, and simplicity of the method.**

***Index Terms*— Electromagnetic (EM), equivalent circuit, model order reduction (MOR), partial element equivalent circuit (PEEC).**

## I. Introduction

THE partial element equivalent circuit (PEEC) model [1] is the only physical meaningful method that converts an electromagnetic (EM) problem into a circuit domain problem, which has been widely adopted in signal integrity analysis, electronic packaging design, EM radiation, EM compatibility, and power electronics problems [2]–[6]. Nevertheless, the PEEC model for a multiconductor structure is a mesh-dependent circuit model, which consists of a large number of *RLC* elements, especially for a practical high-speed or high-frequency circuit. Usually, it is prohibitively time consuming if not possible to directly solve such a large-scale circuit problem because some large-scale matrix inversions are involved. Besides, it is difficult to acquire any physical insight by directly examining the lumped element circuit itself. In recent years, the PEEC model has been used to serve as a good starting point to derive a much more concise and physically meaningful equivalent circuit by the physics-based model order reduction (MOR) technique called derived physically expressive circuit (DPEC) method [7], [8].

A number of mathematics-based MOR techniques have been proposed in the past to generate a low ordered approximation of a large-scale circuit problem, among which are the Lanczos and Arnoldi algorithms that are the subclass of the so-called Krylov subspace iteration methods which constitute the main framework of modern MOR research [9]–[13]. These techniques approximate the system responses by using some matrix operations, such as QR decompositions, LU decompositions, and matrix inversions. These techniques have a good performance for moderate-sized problems. However, the scalability issue is a limiting factor in the applications as they all involve matrix inversions or decompositions. Since the order-reduced macro model involves full matrices in its modified nodal analysis (MNA) state equation, there is no direct physics interpretation from the model.

In this paper, a new mesh-based MOR method that confronts the two major issues faced by the DPEC method is fully presented with extensive theoretical elaboration and practical numerical details. The two issues are: 1) it involves two large matrix inversions, one for obtaining the coefficients of capacitance matrix from the coefficients of potential matrix and the other for converting the mutual inductive couplings into so-called nonphysical direct inductance and 2) the order-reduced circuit model does not reflect physically meaningful mutual inductance as the direct inductances are not reversible to sensible mutual inductances. This first issue limits the scalability of the method and the second issue causes loss the physical meaning of the order-reduced micromodel.

This paper presents the first method that allows deriving a concise and physically meaningful micromodel directly from the mixed potential integral equation (MPIE) and the mesh information on conductor surfaces. Instead of dealing with the capacitances, which must be obtained by a matrix inversion, the proposed method uses the potential coefficients directly. A legitimate circuit transformation, which directly involves mutual inductances and is inspirited from the mesh information, is introduced. It will be shown that this new mesh-based MOR technique neither requires any matrix operations nor introduces any physically meaningless circuit components throughout the MOR process. Recently, a preliminary result of applying this MOR method on a small-size meander delay line circuit was reported in a conference paper [14] with validation by a comparison of results of this method and those of PEEC model. Theories for the following indispensable

Manuscript received October 15, 2015; revised May 8, 2016 and June 20, 2016; accepted June 26, 2016. Date of publication July 21, 2016; date of current version August 4, 2016. This work was supported by the Research Grants Council of the Hong Kong Special Administrative Region, China, under Grant CUHK 417612. This paper is an expanded version from the 2015 IEEE MTT-S International Conference on Numerical Electromagnetic and Multiphysics Modeling and Optimization, Ottawa, ON, Canada, August 2015. *(Corresponding author: Ke-Li Wu.)*

The authors are with the Department of Electronic Engineering, The Chinese University of Hong Kong, Hong Kong (e-mail: yhdou@ee.cuhk.edu.hk; klwu@ee.cuhk.edu.hk).

Color versions of one or more of the figures in this paper are available online at http://ieeexplore.ieee.org.

Digital Object Identifier 10.1109/TMTT.2016.2586057

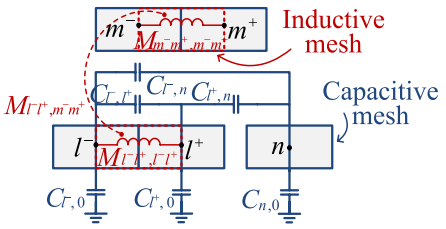


Fig. 1. PEEC meshes together with partial inductances and capacitances.

components in the MOR process will be elaborated in this paper: 1) the low-pass approximation and node selection criterion; 2) combining of two shunt branches that are coupled with all the rest of branches; and 3) the conversion of the mixed coupling between a capacitor and an inductor to a sensible inductive coupling. Three practical examples are investigated in this paper, including a large-scale practical interconnection problem. A comparative study of the proposed method and the well-known Krylov iteration method [10] is conducted in terms of computational complicity, efficiency, and stability in example 3 of Section IV. The comparison further reveals the unique features of this new method and its superiority over the classical method. This paper will focus on the quasi-static high-speed/microwave circuit problems.

## II. Overview of the PEEC Model

### A. PEEC Modeling for Static Problems

The PEEC model is based on the circuit representation of the discretized MPIE [1]. For simplicity, considering an infinitely thin conducting strip, the frequency-domain static PEEC formulation starts from the MPIE

$$\mathbf{E}(\mathbf{r}) = -j\omega \int_{s'} \overline{\overline{G_A}}(\mathbf{r},\mathbf{r}') \cdot \mathbf{J}(\mathbf{r}')ds' - \nabla \int_{s'} G_\varphi(\mathbf{r},\mathbf{r}')\rho(\mathbf{r}')ds' \tag{1}$$

where $\bar{\bar{G}}_A$ and $G_\varphi$ are the dyadic and scalar Green's functions for magnetic vector and electric scalar potentials, respectively, and $\rho$ and $\boldsymbol{J}$ are the surface charges and current densities, respectively.

By dividing a conducting strip into capacitive meshes with charges laid on and inductive meshes with currents flown through, the charge and current densities are discretized. Since these meshes are small enough, charge density of each capacitive mesh and current density of each inductive mesh will be assumed to be a constant. Fig. 1 illustrates that a capacitive mesh needs to be introduced between two or more connected inductive meshes to satisfy the current continuity condition.

In addition, without loss of generality, only the $x$-component in (1) is considered. By separately discretizing the current and charge densities using rectangular pulse functions, applying Galerkin's matching procedure and having $r$ reside on the conducting strip, the discretized form of (1) is given by

$$\frac{l_l}{\sigma w_l} I_l^x + \sum_m \frac{j\omega}{w_l w_m} \left( \iint G_A^{xx}(\mathbf{r},\mathbf{r}')ds'_m ds_l \right) I_m^x + \sum_n \frac{d}{dx}\frac{1}{w_l a_n} \left( \iint G_\varphi(\mathbf{r},\mathbf{r}')ds'_n ds_l \right) Q_n = 0 \tag{2}$$

where mesh $m$ is the inductive mesh and mesh $n$ is the capacitive mesh, $w_l$ and $w_m$ are the widths of inductive meshes $l$ and $m$, respectively, $a_n$ is the area of capacitive mesh $n$. Subscript $l = 1, \ldots, M$ and $M$ is the total number of inductive meshes. It is worth mentioning that (2) is in the form of Kirchhoff's voltage law (KVL). The terms on the left-hand side represent, respectively, the resistive, inductive, and capacitive voltage drops across inductive mesh $l$. In a more circuit-oriented form, (2) can be represented as (superscript $x$ is dropped from now on)

$$R_l I_{l^-l^+} + \sum_m j\omega M_{l^-l^+,m^-m^+} I_{m^-m^+} + \sum_n (pp_{l^+,n} - pp_{l^-,n}) Q_n = 0 \tag{3}$$

where indices $l^-$ and $l^+$ are associated with inductive cell $l$ with current $I_{l^-l^+}$ flowing from node $l^-$ to node $l^+$. Constant $M_{l^-l^+,m^-m^+}$ is the partial (self or mutual) inductance between inductive cells ended by nodes $l^\pm$ and $m^\pm$, respectively. Constant $pp_{l^\pm,n}$ is the coefficient of electric potential between capacitive cells $l^\pm$ and $n$. Constant $Q_n$ is the total charge on the capacitive cell $n$. A finite-difference approximation has been used for the derivative operator in the third term of (2). For ease of analysis, conductor loss $R_l$ is conflated with the corresponding self-inductance $M_{l^-l^+,l^-l^+}$, and (3) becomes

$$\sum_m j\omega M_{l^-l^+,m^-m^+} I_{m^-m^+} + \sum_n (pp_{l^+,n} - pp_{l^-,n}) Q_n = 0. \tag{4}$$

### B. Basic Circuit Element of PEEC

Conventionally, for a multiple conductor circuit, the self-partial capacitance $C_{i,0}$ of capacitive mesh $i$ and mutual partial capacitance $C_{i,j}$ between capacitive meshes $i$ and $j$ can be obtained from coefficients of potential matrix $[pp]$ in (4). Inverting these coefficients of potential matrix, one can get the *coefficient of capacitance* $c_{i,i}$ and *coefficient of induction* $c_{i,j}$ by

$$[c]_{N\times N} = [pp]^{-1}_{N\times N}. \tag{5}$$

The actual self-partial and mutual partial capacitances [15] can be obtained by

$$C_{i,0} = \sum_{j=1}^{N} c_{i,j} \text{ and } C_{i,j} = -c_{i,j} (i \neq j). \tag{6}$$

Therefore, KVL equation (4) can be illustrated as circuit in Fig. 1. A self-partial inductance $M_{l^-l^+,l^-l^+}$ of inductive mesh $l$ incorporates mutual inductive coupling $M_{l^-l^+,m^-m^+}$ with every self-partial inductance $M_{m^-m^+,m^-m^+}$ of inductive mesh $m$. At its two end capacitive meshes $l^\pm$, self-partial capacitances $C_{l^\pm,0}$ and mutual partial capacitances with every capacitive mesh $n$, capacitances $C_{l^\pm,n}$, exist.

### C. Potances of Capacitive Couplings

As stated above, coefficients of potential for a multiconductor system can fully represent the partial capacitances.

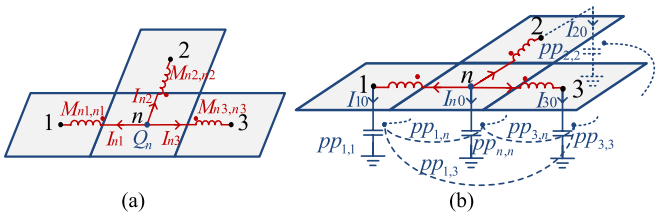


Fig. 2. Illustration of potor current. (a) Currents of inductive meshes and charges of capacitive meshes. (b) Self- and mutual partial inductances and potances.

Therefore, it is not necessary to convert coefficients of potential to partial capacitances, which requires inverting a large matrix for circuit analysis, or as required in a physics-based MOR as done in [7] and [8]. Directly dealing with coefficients of potential can avoid inverting a large-scale matrix of coefficients of potential.

As analogous to conventional definitions of self-inductance of an inductor and mutual inductance of two inductors, for convenience, quantity $pp_{i,i}$ is called *self-potance* of the circuit element *potor* and $pp_{i,j}$ is called *mutual potance* of two *potors*. As illustrated by the mesh schematic in Fig. 2(a), the charge $Q_n$ of capacitive mesh $n$ and the currents $I_{ni}$ ($i = 1, 2, 3$) of its connected inductors $M_{ni,ni}$ follow the current continuity equation

$$-j\omega Q_n = \sum_{i=1}^{3} I_{ni}. \tag{7}$$

The circuit representation of this example with inductances and potances is shown in Fig. 2(b), where $I_{n0}$ is the current flowing through potor $pp_{n,n}$ of node $n$ to ground and satisfies the following relation:

$$I_{n0} = j\omega Q_n. \tag{8}$$

By using (8) in (7), one can obtain a Kirchhoff's current law (KCL) equation for the circuit

$$\sum_{i=0}^{3} I_{ni} = 0. \tag{9}$$

Using (9) in KVL equation (4) yields

$$\sum_{m} j\omega M_{l^-l^+,m^-m^+} I_{m^-m^+} + \sum_{n} \left( \frac{pp_{l^+,n}}{j\omega} I_{n0} - \frac{pp_{l^-,n}}{j\omega} I_{n0} \right) = 0. \tag{10}$$

Equation (10) can be well interpreted by the circuit shown in Fig. 3. The equation reveals that the voltage from node $l^{\pm}$ to ground or $V_{l^{\pm}0}$ , of inductive mesh $l$ can be expressed as

$$V_{l^{\pm}0} = \sum_{n} \frac{pp_{l^{\pm},n}}{j\omega} I_{n0} = \frac{pp_{l^{\pm},l^{\pm}}}{j\omega} I_{l^{\pm}0} + \sum_{n \neq l^{\pm}} \frac{pp_{l^{\pm},n}}{j\omega} I_{n0} \tag{11}$$

which states that the voltage $V_{l^{\pm}0}$ of capacitive mesh $l^{\pm}$ is caused by both self-potance $pp_{l^{\pm},l^{\pm}}$ and mutual potance $pp_{l^{\pm},n}$.

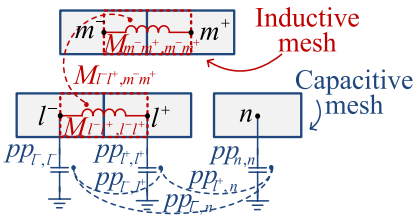


Fig. 3. Circuit interpretation of KVL equation using potors and inductors.

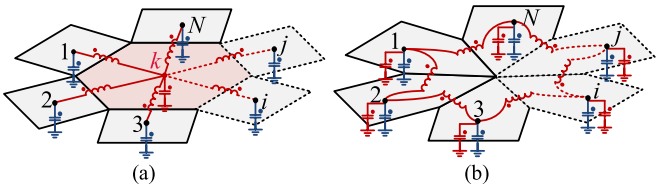


Fig. 4. Representative meshes prior and posterior to the transformation for absorbing node $k$. (a) Meshes prior to transformation. (b) Equivalent meshes posterior to transformation.

Although the PEEC model can be solved using a circuit solver, for a circuit that involves a large number of circuit elements and branches, the computing time can be prohibitively long. Therefore, it is highly desirable to have the order of the circuit model reduced before finding the circuit responses. This demand has impelled tremendous research activities in searching for effective MOR techniques that possess two desired attributes: 1) the order of the original circuit model is reduced by a few orders of magnitude and 2) the order-reduced circuit model contains as much physical essence of the original EM problem as possible.

## III. Theory

The main idea of the proposed method is to absorb the contribution, based on a generalized Y-Δ circuit transformation, from all the insignificant internal nodes in a PEEC model recursively while retaining the essence of its physical meaning in the low-pass sense. The progressive process will be stopped when a prescribed low-pass approximation criterion is no longer satisfied.

### A. Hypothesis of Mesh-Based Circuit Transformation

It is intuitive to explain the transformation by examining the exemplary mesh arrangement shown in Fig. 4(a). Assume that node $k$, which corresponds to capacitive mesh $k$, is an insignificant node to be absorbed. The transformed circuit together with its corresponding mesh arrangement, after node $k$ being absorbed, is hypothesized to be the one shown in Fig. 4(b), in which capacitive contribution of mesh $k$ is uniformly distributed to the $N$ capacitive meshes that are originally adjacent to mesh $k$. It is believed that with the following five updating rules in the transformation, the circuit properties of the transformed circuit will be retained.

1) The original grounded potance $pp_{k,k}$ and the $N$ inductors that were originally connected to node $k$ are absorbed.

2) An incremental grounded potor is added to the original potor of each originally adjacent capacitive mesh to reflect the newly added one-$N$th of portion of capacitive mesh $k$.
3) A new inductor is introduced between each consecutive pair of newly updated adjacent capacitive meshes.
4) All the mutual couplings between the absorbed elements are transferred to the mutual couplings between the newly introduced elements.
5) All the mutual couplings between the absorbed elements and remaining circuit elements are transferred to the mutual couplings between the newly introduced elements and the remaining circuit elements.

For clarity, hereinafter, inductive couplings are represented by circular dots and capacitive couplings are represented by square dots. The artificial mutual coupling between an inductor and a capacitor, which is named as mixed coupling, will be introduced for convenience and is represented by a triangular dot.

In the following, the theory of the circuit transformation is developed. For the convenience of mathematical description, assuming that node $k$ is to be absorbed, the notation assignments are as follows.

1) Terminals of the remaining elements are numbered $1, 2, \ldots, m, \ldots, n, \ldots, s, \ldots, t, \ldots, M$.
2) Terminals of the removed elements and newly introduced elements are numbered $1, 2, \ldots, i, \ldots, j, \ldots, N$ counted clockwise or counterclockwise along the contour of mesh $k$.
3) Adjacent nodes of node $k$ can be terminals of both remaining and newly introduced elements. For example, in Fig. 5, terminal $i$ for newly introduced elements and terminal $s$ for remaining elements represent the same node.
4) Index 0 represents the ground.
5) Superscript $k$ represents the circuit updating related to absorbing node $k$.

The above conventions can be well illustrated by the representative circuit shown in Fig. 5.

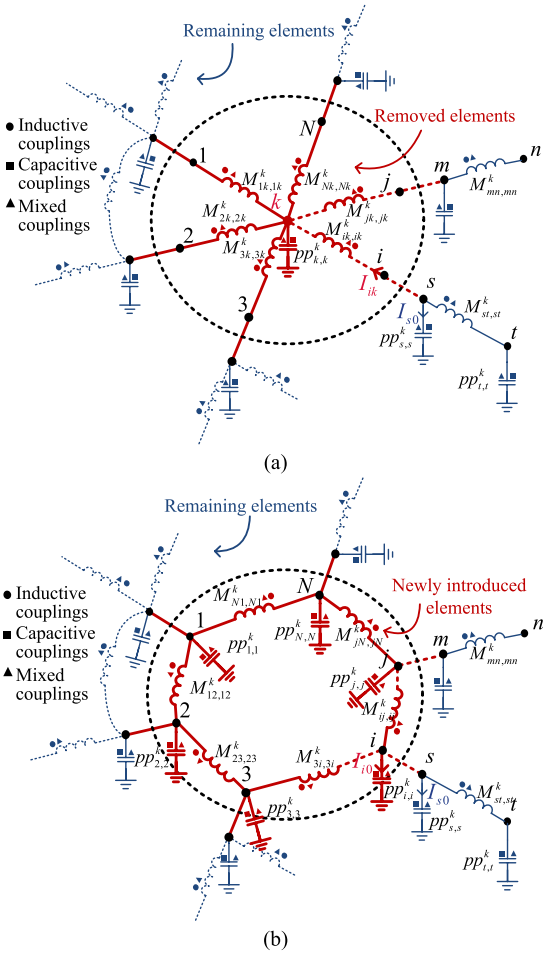


Fig. 5. Equivalent circuit transformation of absorbing node $k$. (a) Circuit prior to transformation. (b) Circuit posterior to transformation.

### B. Equivalence Conditions of Circuit Transformation

Traditionally, equivalent circuit transformation should satisfy the conditions in which voltage–current relations related to node $k$ remain the same. Since the charge on original mesh $k$ needs to be divided into $N$ equal parts, an incremental current to ground, which is equal to $N$ fraction of the current through original potor $k$, needs to be introduced to each newly added potor. Referring to Fig. 5(a) and (b), the equivalence conditions for the circuit transformation are imposed, which are as follows.

1) Voltages and currents for the newly introduced elements must satisfy the following KVL equations:

$$V_{i0}^k = V_{ik}^k + V_{k0}^k \quad (i = 1, \ldots, N) \tag{12a}$$

$$V_{i(i+1)}^k = V_{ik}^k - V_{(i+1)k}^k \tag{12b}$$

where

$$V_{(N+1)k}^k = V_{1k}^k, \quad V_{0k}^k = V_{Nk}^k$$

and the KCL equation

$$I_{ik}^k = I_{i(i+1)}^k - I_{(i-1)i}^k + I_{i0}^k \tag{13}$$

where $I_{i0}^k = I_{k0}^k/N$, $I_{N(N+1)}^k = I_{01}^k = I_{N1}^k$.

2) Voltages and currents for the remaining elements are unchanged.

### C. Mixed Coupling Elements

To update the elements related to newly added potor $pp_{i,i}^k$ in Fig. 5(b), the voltage across the potor can be expressed in terms of branch currents posterior to the transformation. According to KVL equation (12a) and the linear superposition principle, the voltage $V_{i0}^k$ can be obtained from the circuit prior to the transformation in Fig. 5(a) as

$$V_{i0}^k = \frac{pp_{k,k}^k}{j\omega} I_{k0}^k + \sum_s \frac{pp_{k,s}^k}{j\omega} I_{s0}^k + \sum_{j=1}^N j\omega M_{ik,jk}^k I_{jk}^k + \sum_{(m,n)} j\omega M_{ik,mn}^k I_{mn}^k \tag{14}$$

where *(m, n)* is a combined index referring to the pair of nodes at the two ends of inductor $M_{mn,mn}$. Using KCL equation (13), (14) becomes

$$\begin{aligned} V_{i0}^k &= \frac{pp_{k,k}^k}{j\omega} N I_{i0}^k + \sum_s \frac{pp_{k,s}^k}{j\omega} I_{s0}^k \\ &\quad + \sum_{j=1}^{N} j\omega M_{ik,jk}^k \left(I_{j(j+1)}^k - I_{(j-1)j}^k + I_{j0}^k\right) \\ &\quad + \sum_{(m,n)} j\omega M_{ik,mn}^k I_{mn}^k \\ &= \frac{pp_{i,i}^k}{j\omega} I_{i0}^k + \sum_{j=1, j\neq i}^{N} \frac{pp_{i,j}^k}{j\omega} I_{j0}^k + \sum_s \frac{pp_{i,s}^k}{j\omega} I_{s0}^k \\ &\quad + \sum_{j=1}^{N} j\omega X_{i,j(j+1)}^k I_{j(j+1)}^k + \sum_{(m,n)} j\omega X_{i,mn}^k I_{mn}^k \end{aligned} \tag{15}$$

where

$$\begin{aligned} &\sum_{j=1}^{N} j\omega M_{ik,jk}^k I_{(j-1)j}^k \\ &\quad = j\omega M_{ik,1k}^k I_{01}^k + \sum_{j=2}^{N} j\omega M_{ik,jk}^k I_{(j-1)j}^k \\ &\quad = j\omega M_{ik,(N+1)k}^k I_{N(N+1)}^k + \sum_{j=1}^{N-1} j\omega M_{ik,(j+1)k}^k I_{j(j+1)}^k \\ &\quad = \sum_{j=1}^{N} j\omega M_{ik,(j+1)k}^k I_{j(j+1)}^k \end{aligned} \tag{16}$$

and

$$\begin{aligned} pp_{i,i}^k &= N pp_{k,k}^k - \omega^2 M_{ik,ik}^k, \quad pp_{i,j}^k = -\omega^2 M_{ik,jk}^k \\ pp_{i,s}^k &= pp_{k,s}^k \\ X_{i,j(j+1)}^k &= M_{ik,jk}^k - M_{ik,(j+1)k}^k, \quad X_{i,mn}^k = M_{ik,mn}^k. \end{aligned} \tag{17}$$

It is seen that the voltage across a newly added potor is contributed by five types of currents: 1) the current through the new potor; 2) the currents through other newly added potors; 3) the currents through the remaining potors; 4) the currents flowing through the newly introduced inductors; and 5) the currents flowing through all the remaining inductors, respectively, according to the order of the terms appearing in the last expression in (15). For the convenience of a general description, a mixed coupling $X_{i,mn}^k$, which is basically a linear combination of inductive couplings, is *temporally* introduced in (17) to represent the contribution to the voltage across potor $i$ from the inductor $M_{mn,mn}^k$ after node $k$ is absorbed.

Similarly, to update the elements related to newly introduced inductor $M_{i(i+1),i(i+1)}^k$ in Fig. 5(b), applying KVL equation (12b) and the linear superposition principle, the voltage $V_{i(i+1)}^k$ can be obtained as

$$\begin{aligned} V_{i(i+1)}^k &= V_{ik}^k - V_{(i+1)k}^k \\ &= \left(\sum_{j=1}^{N} j\omega M_{ik,jk}^k I_{jk}^k + \sum_{(m,n)} j\omega M_{ik,mn}^k I_{mn}\right) \\ &\quad - \left(\sum_{j=1}^{N} j\omega M_{(i+1)k,jk}^k I_{jk}^k + \sum_{(m,n)} j\omega M_{(i+1)k,mn}^k I_{mn}\right). \end{aligned} \tag{18}$$

Using KCL equation (13), (18) becomes

$$\begin{aligned} V_{i(i+1)}^k &= \sum_{j=1}^{N} j\omega \left(M_{ik,jk}^k - M_{ik,(j+1)k}^k - M_{(i+1)k,jk}^k \right. \\ &\qquad \left. + M_{(i+1)k,(j+1)k}^k\right) I_{j(j+1)}^k \\ &\quad + \sum_{j=1}^{N} j\omega \left(M_{ik,jk}^k - M_{(i+1)k,jk}^k\right) I_{j0}^k \\ &\quad + \sum_{(m,n)} j\omega \left(M_{ik,mn}^k - M_{(i+1)k,mn}^k\right) I_{mn} \\ &= \sum_{j=1}^{N} j\omega M_{i(i+1),j(j+1)}^k I_{j(j+1)}^k + \sum_{j=1}^{N} j\omega X_{j,i(i+1)}^k I_{j0}^k \\ &\quad + \sum_{(m,n)} j\omega M_{i(i+1),mn}^k I_{mn} \end{aligned} \tag{19}$$

where

$$\begin{aligned} M_{i(i+1),j(j+1)}^k &= M_{ik,jk}^k - M_{ik,(j+1)k}^k - M_{(i+1)k,jk}^k \\ &\quad + M_{(i+1)k,(j+1)k}^k \\ X_{j,i(i+1)}^k &= M_{ik,jk}^k - M_{(i+1)k,jk}^k \\ M_{i(i+1),mn}^k &= M_{ik,mn}^k - M_{(i+1)k,mn}^k. \end{aligned} \tag{20}$$

It is seen that the voltage across a newly introduced inductor is contributed by three types of currents: 1) the currents flowing through the newly introduced inductors; 2) the currents flowing through newly added potors; and 3) the currents flowing through all the remaining inductors, respectively, according to the order of the terms appearing in the last expression in (19). The mixed coupling $X_{j,i(i+1)}^k$ temporally introduced in (20) represents the contribution to the voltage across the inductor $M_{i(i+1),i(i+1)}^k$ from potor $j$ after node $k$ is absorbed.

### D. General Y-Δ Circuit Transformation

With the same methodology as that used in the above section, a general Y-Δ transformation of a PEEC circuit containing inductive, capacitive, and mixed coupling elements can be derived for absorbing node $k$. The detailed derivation is given in Appendix I, but the complete element updating formulas are given here.

1) For newly added elements

$$pp^k_{i,i} = Npp^k_{k,k} - \omega^2\left(M^k_{ik,ik} + 2X^k_{k,ik}\right) \quad (21)$$

$$pp^k_{i,j} = -\omega^2\left(M^k_{ik,jk} + X^k_{k,ik} + X^k_{k,jk}\right) \quad (22)$$

$$M^k_{i(i+1),j(j+1)} = M^k_{ik,jk} - M^k_{ik,(j+1)k} - M^k_{(i+1)k,jk} + M^k_{(i+1)k,(j+1)k} \quad (23)$$

$$X^k_{i,j(j+1)} = M^k_{ik,jk} + X^k_{k,jk} - M^k_{ik,(j+1)k} - X^k_{k,(j+1)k}. \quad (24)$$

2) For couplings among newly added elements and the remaining elements

$$pp^k_{i,s} = pp^k_{k,s} - \omega^2 X^k_{s,ik} \quad (25)$$

$$M^k_{i(i+1),mn} = M^k_{ik,mn} - M^k_{(i+1)k,mn} \quad (26)$$

$$X^k_{i,mn} = M^k_{ik,mn} + X^k_{k,mn} \quad (27a)$$

$$X^k_{s,i(i+1)} = X^k_{s,ik} - X^k_{s,(i+1)k}. \quad (27b)$$

3) Couplings among remaining elements remain the same.

The transformed circuit contains three nonconformities with the basic PEEC circuit configuration.

1) The potances updated by (21), (22), and (25) are frequency dependent.
2) Each newly added potor is in shunt with a remaining potor, e.g., $pp^k_{i,i}$ is in shunt with $pp^k_{s,s}$; and a newly introduced inductor may be in shunt with a remaining inductor, e.g., $M^k_{ij,ij}$ and $M^k_{ms,ms}$ are in shunt, as illustrated in Fig. 5(b).
3) Mixed couplings exist.

The first two nonconformities need to be remedied before moving forward to absorbing the next insignificant node, whereas the last nonconformity will be corrected after all the insignificant nodes are absorbed.

### *E. Low-Pass Approximation*

The frequency-dependent part of potances (21), (22), and (25) is introduced in the general Y-$\Delta$ circuit transformation. Since the voltage across potor $pp^k_{i,i}$ is equal to the sum of the voltage across the removed inductor $M^k_{ik,ik}$ and that of potor $pp^k_{k,k}$, as illustrated in Fig. 5(a), the impedance of the potor can be considered as an *LC* series resonator. For most of the high-speed circuit problems, people are interested in the characteristics of an equivalent circuit from dc to a designated cutoff frequency. Therefore, applying a legitimate low-pass approximation to the transformed circuit will lead to a simplified circuit model containing the essence of the original circuit in the low-pass sense.

For the self-potance given by (21), its impendence can be expressed by

$$Z^k_{i,i} = Npp^k_{k,k}/j\omega + j\omega\left(M^k_{ik,ik} + 2X^k_{k,ik}\right) \quad (28)$$

where the first term represents a capacitive contribution and the second term represents an inductive contribution. With the following low-pass condition satisfied:

$$\left|\frac{j\omega_{\max}\left(M^k_{ik,ik} + 2X^k_{k,ik}\right)}{Npp^k_{k,k}/j\omega_{\max}}\right| = \left|\frac{\omega^2_{\max}\left(M^k_{ik,ik} + 2X^k_{k,ik}\right)}{Npp^k_{k,k}}\right| \ll 1 \quad (29)$$

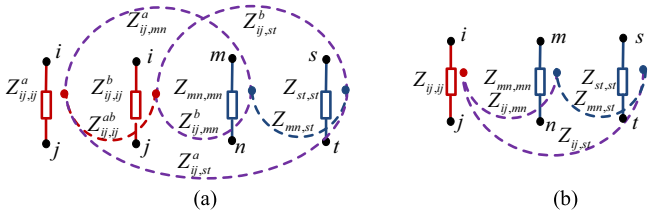


Fig. 6. Combining process of two coupled shunt elements. (a) Circuit prior to combining. (b) Circuit posterior to combining.

which means that the capacitive component is much more dominant than the inductive component, the self-potance $pp^k_{i,i}$ can be approximated by a frequency-independent potance with

$$pp^k_{i,i} = Npp^k_{k,k} \quad (30)$$

where $\omega_{\max}$ is the cutoff frequency of the low-pass approximation. By the same token, with the low-pass conditions specified by

$$\left|\frac{\omega^2_{\max}\left(M^k_{ik,jk} + X^k_{k,ik} + X^k_{k,jk}\right)}{Npp^k_{k,k}}\right| \ll 1 \text{ and } \left|\frac{\omega^2_{\max}X^k_{s,jk}}{Npp^k_{k,k}}\right| \ll 1 \quad (31)$$

satisfied, mutual potance $pp^k_{i,j}$ and $pp^k_{i,s}$ can be approximated by two constants

$$pp^k_{i,j} = 0, \quad pp^k_{i,s} = pp^k_{k,s}. \quad (32)$$

Because self-inductance $M^k_{ik,ik}$ is usually much larger than mutual inductance and mixed couplings that are caused by mutual inductances, when condition (29) is satisfied, conditions in (31) will be automatically satisfied. Therefore, it is assured that if a node meets the following condition, it can be absorbed by the transformation with the low-pass approximation:

$$\left|\omega^2_{\max}\left(M^k_{ik,ik} + 2X^k_{k,ik}\right)/Npp^k_{k,k}\right| < \delta. \quad (33)$$

In other words, its contribution to the circuit attributes in the specified low-pass frequency range is insignificant, where criterion $\delta$ is specified to control the approximation accuracy. With the low-pass approximation, the Y-$\Delta$ circuit transformation can directly generate a frequency-independent circuit model which is conformal to the basic PEEC circuit configuration with a specified accuracy.

### *F. Combining Two Coupled Shunt Elements*

It has been shown that having absorbed a node all the newly generated circuit elements in the transformed circuit may be shunt connected to surrounding elements. However, these shunt connected elements incorporate mutual couplings with all the circuit elements, which must be combined before moving to absorbing next node.

Combining two shunt elements of the same type (inductors or potors) will not only the couplings with combined element themselves but also influence all the couplings among all other circuit elements slightly. The general process of combining two shunt elements between nodes $i$ and $j$ is illustrated by Fig. 6.

By the linear superposition principle, the currents flowing through the two shunt connected elements can be solved as

$$\begin{pmatrix} I_{ij}^a \\ I_{ij}^b \end{pmatrix} = \begin{pmatrix} Z_{ij,ij}^a & Z_{ij,ij}^{ab} \\ Z_{ij,ij}^{ab} & Z_{ij,ij}^b \end{pmatrix}^{-1} \times \left\{ \begin{pmatrix} V_{ij}^a \\ V_{ij}^b \end{pmatrix} - \begin{pmatrix} \sum\limits_{(m,n)} Z_{ij,mn}^a I_{mn} \\ \sum\limits_{(m,n)} Z_{ij,mn}^b I_{mn} \end{pmatrix} \right\}. \quad (34)$$

Because $I_{ij} = I_{ij}^a + I_{ij}^b$ and $V_{ij} = V_{ij}^a = V_{ij}^b$, the relation between $I_{ij}$ and $V_{ij}$ can be found to be

$$V_{ij} = \frac{1}{Y_t} I_{ij} + \sum_{(m,n)} \frac{\left(Y_{ij,ij}^a + Y_{ij,ij}^{ab}\right) Z_{ij,mn}^a + \left(Y_{ij,ij}^b + Y_{ij,ij}^{ab}\right) Z_{ij,mn}^b}{Y_t} I_{mn} \quad (35)$$

where

$$\begin{pmatrix} Y_{ij,ij}^a & Y_{ij,ij}^{ab} \\ Y_{ij,ij}^{ab} & Y_{ij,ij}^b \end{pmatrix} = \begin{pmatrix} Z_{ij,ij}^a & Z_{ij,ij}^{ab} \\ Z_{ij,ij}^{ab} & Z_{ij,ij}^b \end{pmatrix}^{-1}$$

and

$$Y_t = Y_{ij,ij}^a + Y_{ij,ij}^b + 2Y_{ij,ij}^{ab}. \quad (36)$$

Hence, the self-impedance and the direct mutual impedance can be obtained as

$$Z_{ij} = 1/Y_t \quad (37)$$

$$Z_{ij,mn} = \left[\left(Y_{ij,ij}^a + Y_{ij,ij}^{ab}\right) Z_{ij,mn}^a + \left(Y_{ij,ij}^b + Y_{ij,ij}^{ab}\right) Z_{ij,mn}^b\right] / Y_t. \quad (38)$$

Consequently, the other branch voltage $V_{mn}$ across nodes $m$ and $n$ is also related to branch currents $I_{ij}^a$ and $I_{ij}^b$ by

$$V_{mn} = Z_{ij,mn}^a I_{ij}^a + Z_{ij,mn}^b I_{ij}^b + \sum_{(s,t)} Z_{mn,st} I_{st}. \quad (39)$$

By using (34) and (35) in (39), as derived in (A-13), the indirect self-impedance or mutual impedance $Z_{mn,st}$ will be updated by

$$Z_{mn,st} = Z_{mn,st} - \frac{Y_{ij,ij}^a Y_{ij,ij}^b - \left(Y_{ij,ij}^{ab}\right)^2}{Y_t} \times \left(Z_{ij,mn}^a - Z_{ij,mn}^b\right)\left(Z_{ij,st}^a - Z_{ij,st}^b\right). \quad (40)$$

For different types of elements and different types of mutual couplings, including the mixed type of mutual coupling elements, the specific expressions for updating elements are different. The detailed updating formulas are given in Table I.

At this point, the PEEC model, consisting of frequency-independent potances, inductances, as well as mixed couplings, has been approximated by a new simplified PEEC model with the same constitution but one insignificant node absorbed, in the low-pass sense. This process can be repeated until no more nodes satisfy the low-pass criterion.

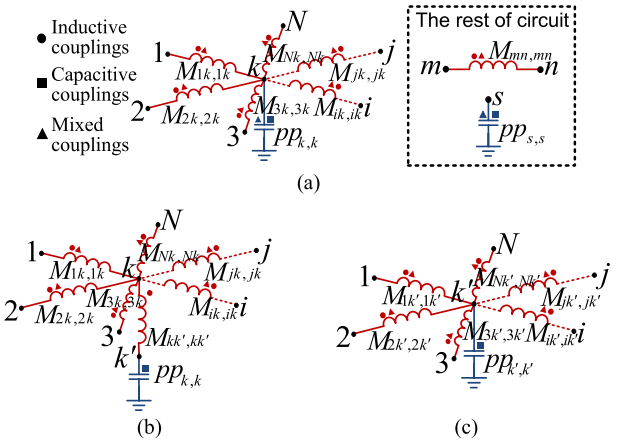


Fig. 7. Progress of converting mixed couplings into inductive couplings. (a) Potor $k$ with mixed couplings. (b) Mixed couplings replaced by inductive couplings. (c) Potor $k'$ without mixed couplings.

### G. Mixed Coupling to Inductive Coupling Transformation

Mixed coupling is introduced to count the voltage across an element which is contributed by the current flowing through another type of element. It can be absorbed by the inductors serially connected to this potor.

A typical mixed coupling circuit related to potor $pp_{k,k}$ is illustrated in Fig. 7(a). A potor that has mixed couplings can be equivalently replaced by a new potor that does not have any mixed coupling in series with an inductor that is coupled to the original potor's mixed coupled inductors as illustrated in Fig. 7(b). Potor $pp_{k,k}$ is replaced by potor $pp_{k',k'}$ in series with an inductor $M_{kk',kk'}$. In this equivalence, inductor $M_{kk',kk'}$ only has mutual inductive couplings with other inductors, and potor $pp_{k',k'}$ only has mutual capacitive couplings with other potors. Then the inductor $M_{kk',kk'}$ can be merged with inductors $M_{ik,ik}$ as $M_{ik',ik'}$ as shown in Fig. 7(c), where $i = 1, 2, \ldots, N$. Obviously, potor $pp_{k',k'}$ inherits the capacitive part of potor $pp_{k,k}$, that is,

$$pp_{k',k'} = pp_{k,k}, \quad pp_{k',s} = pp_{k,s}. \quad (41)$$

For the new inductor $M_{kk',kk'}$, since

$$V_{ik'} = V_{ik} + V_{kk'} = \sum_{j=1}^{N} j\omega(M_{ik,jk} + X_{k,ik} + X_{k,jk}) I_{jk} + \sum_{(m,n)} j\omega(M_{ik,mn} + X_{k,mn}) I_{mn} + \sum_{s} j\omega X_{s,ik} I_{s0} \quad (42)$$

the mutual inductive couplings with the new transformed inductor $M_{kk',kk'}$ can be found as follows.

1) For inductive couplings with transformed inductors

$$M_{ik',jk'} = M_{ik,jk} + X_{k,ik} + X_{k,jk}. \quad (43)$$

2) For inductive couplings with the rest of the inductors

$$M_{ik',mn} = M_{ik,mn} + X_{k,mn}. \quad (44)$$

It can be noted that nodes $k'$ and $k$ represent the same node after the transformation. A circuit without mixed couplings can be obtained after every potor being transformed.

TABLE I

ELEMENTS UPDATING EQUATIONS FOR COMBINING TWO COUPLED POTORS AND INDUCTORS

| | | |
|---|---|---|
| 1. | 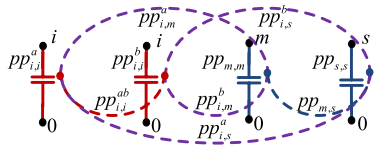 | $pp_{i,i}=[pp^a_{i,i}pp^b_{i,i}-(pp^{ab}_{i,i})^2]/(pp^a_{i,i}+pp^b_{i,i}-2pp^{ab}_{i,i})$<br>$pp_{i,m}=[(pp^b_{i,i}-pp^{ab}_{i,i})pp^a_{i,m}+(pp^a_{i,i}-pp^{ab}_{i,i})pp^b_{i,m}]/(pp^a_{i,i}+pp^b_{i,i}-2pp^{ab}_{i,i})$<br>$pp_{m,s}=pp_{m,s}-(pp^a_{i,m}-pp^b_{i,m})(pp^a_{i,s}-pp^b_{i,s})/(pp^a_{i,i}+pp^b_{i,i}-2pp^{ab}_{i,i})$ |
| 2. | 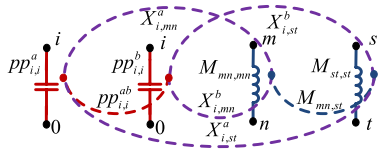 | $pp_{i,i}=[pp^a_{i,i}pp^b_{i,i}-(pp^{ab}_{i,i})^2]/(pp^a_{i,i}+pp^b_{i,i}-2pp^{ab}_{i,i})$<br>$X_{i,mn}=[(pp^b_{i,i}-pp^{ab}_{i,i})X^a_{i,mn}+(pp^a_{i,i}-pp^{ab}_{i,i})X^b_{i,mn}]/pp^a_{i,i}+pp^b_{i,i}-2pp^{ab}_{i,i}$<br>$M_{mn,st}=M_{mn,st}-\omega_0^2(X^a_{i,mn}-X^b_{i,mn})(X^a_{i,st}-X^b_{i,st})/(pp^a_{i,i}+pp^b_{i,i}-2pp^{ab}_{i,i})=M_{mn,st}$ |
| 3. | 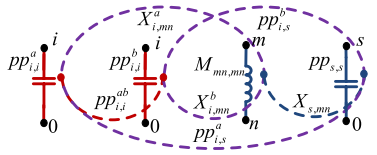 | $pp_{i,i}=[pp^a_{i,i}pp^b_{i,i}-(pp^{ab}_{i,i})^2]/(pp^a_{i,i}+pp^b_{i,i}-2pp^{ab}_{i,i})$,<br>$pp_{i,s}=[(pp^b_{i,i}-pp^{ab}_{i,i})pp^a_{i,s}+(pp^a_{i,i}-pp^{ab}_{i,i})pp^b_{i,s}]/(pp^a_{i,i}+pp^b_{i,i}-2pp^{ab}_{i,i})$<br>$X_{i,mn}=[(pp^b_{i,i}-pp^{ab}_{i,i})X^a_{i,mn}+(pp^a_{i,i}-pp^{ab}_{i,i})X^b_{i,mn}]/(pp^a_{i,i}+pp^b_{i,i}-2pp^{ab}_{i,i})$<br>$pp_{s,s}=pp_{s,s}-(pp^a_{i,s}-pp^b_{i,s})^2/(pp^a_{i,i}+pp^b_{i,i}-2pp^{ab}_{i,i})$<br>$M_{mn,mn}=M_{mn,mn}-[\omega_0^2(X^a_{i,mn}-X^b_{i,mn})^2]/(pp^a_{i,i}+pp^b_{i,i}-2pp^{ab}_{i,i})=M_{mn,mn}$<br>$X_{s,mn}=X_{s,mn}-(X^a_{i,mn}-X^b_{i,mn})(pp^a_{i,s}-pp^b_{i,s})/(pp^a_{i,i}+pp^b_{i,i}-2pp^{ab}_{i,i})$ |
| 4. | 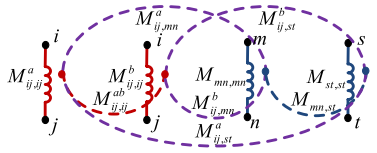 | $M_{ij,ij}=[M^a_{ij,ij}M^b_{ij,ij}-(M^{ab}_{ij,ij})^2]/(M^a_{ij,ij}+M^b_{ij,ij}-2M^{ab}_{ij,ij})$<br>$M_{ij,mn}=[(M^b_{ij,ij}-M^{ab}_{ij,ij})M^a_{ij,mn}+(M^a_{ij,ij}-M^{ab}_{ij,ij})M^b_{ij,mn}]/(M^a_{ij,ij}+M^b_{ij,ij}-2M^{ab}_{ij,ij})$<br>$M_{mn,st}=M_{mn,st}-(M^a_{ij,mn}-M^b_{ij,mn})(M^a_{ij,st}-M^b_{ij,st})/(M^a_{ij,ij}+M^b_{ij,ij}-2M^{ab}_{ij,ij})$ |
| 5. | 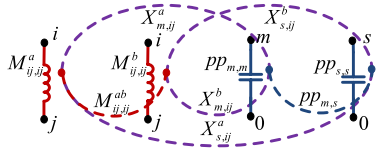 | $M_{ij,ij}=[M^a_{ij,ij}M^b_{ij,ij}-(M^{ab}_{ij,ij})^2]/(M^a_{ij,ij}+M^b_{ij,ij}-2M^{ab}_{ij,ij})$<br>$X_{s,ij}=[(M^b_{ij,ij}-M^{ab}_{ij,ij})X^a_{s,ij}+(M^a_{ij,ij}-M^{ab}_{ij,ij})X^b_{s,ij}]/(M^a_{ij,ij}+M^b_{ij,ij}-2M^{ab}_{ij,ij})$<br>$pp_{m,s}=pp_{m,s}+\omega_0^2(X^a_{m,ij}-X^b_{m,ij})(X^a_{s,ij}-X^b_{s,ij})/(M^a_{ij,ij}+M^b_{ij,ij}-2M^{ab}_{ij,ij})=pp_{m,s}$ |
| 6. | 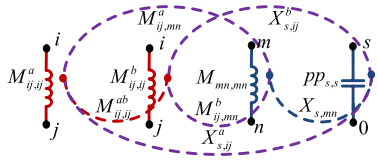 | $M_{ij,ij}=[M^a_{ij,ij}M^b_{ij,ij}-(M^{ab}_{ij,ij})^2]/(M^a_{ij,ij}+M^b_{ij,ij}-2M^{ab}_{ij,ij})$<br>$M_{ij,mn}=[(M^b_{ij,ij}-M^{ab}_{ij,ij})M^a_{ij,mn}+(M^a_{ij,ij}-M^{ab}_{ij,ij})M^b_{ij,mn}]/(M^a_{ij,ij}+M^b_{ij,ij}-2M^{ab}_{ij,ij})$<br>$X_{s,ij}=[(M^b_{ij,ij}-M^{ab}_{ij,ij})X^a_{s,ij}+(M^a_{ij,ij}-M^{ab}_{ij,ij})X^b_{s,ij}]/(M^a_{ij,ij}+M^b_{ij,ij}-2M^{ab}_{ij,ij})$<br>$M_{mn,mn}=M_{mn,mn}-(M^a_{ij,mn}-M^b_{ij,mn})^2/(M^a_{ij,ij}+M^b_{ij,ij}-2M^{ab}_{ij,ij})$<br>$pp_{s,s}=pp_{s,s}+\omega_0^2(X^a_{s,ij}-X^b_{s,ij})^2/(M^a_{ij,ij}+M^b_{ij,ij}-2M^{ab}_{ij,ij})=pp_{s,s}$<br>$X_{s,mn}=X_{s,mn}-(M^a_{ij,mn}-M^b_{ij,mn})(X^a_{s,ij}-X^b_{s,ij})/(M^a_{ij,ij}+M^b_{ij,ij}-2M^{ab}_{ij,ij})$ |

Having reached the end of the MOR process, it is customary that a physically meaningful circuit model will only contain capacitances and inductances. It is straightforward to translate the circuit consisting of potors into a physically meaningful circuit model that only consists of capacitors, capacitive couplings, inductors, and inductive couplings by inverting the potance matrix (coefficients of potential matrix) as described by (5) and (6). It can be noted that the size of the final coefficients of potential matrix will be significantly smaller compared with that of the original PEEC model. Certainly, the potances can also be directly used in frequency domain analysis or as controlled sources in time-domain simulation.

The pseudocode of the proposed direct mesh-based MOR process is summarized in Table II.

### *H. Analysis of Computational Overhead*

Three types of computation are involved in the proposed MOR method: 1) node-absorbing circuit transformation; 2) conversion of the mixed couplings into inductive couplings; and 3) combining coupled shunt elements.

Assuming that the total number of nodes and branches of the original circuit is $N$, the number of nodes and the number of inductors of the final order-reduced circuit are $N_f$ and $N_{lf}$, respectively, the total number of nodes and branches when absorbing a node is $n$, and the number of nodes adjacent to the node to be absorbed is $m$.

The computational overhead for the circuit transformations is $O(N^2)$ and that for converting mixed couplings to inductive coupling is $2N_{lf}^2$, both of which are small enough to be ignored. However, the combining process of coupled shunt elements updates all the mutual couplings of the circuit in absorbing each node using (40). This process can be abstracted as a special outer product as

$$\mathbf{A}=\mathbf{A}+c\mathbf{x}\cdot\mathbf{x}^{\mathbf{T}} \tag{45}$$

where the dimension of column vector $\mathbf{x}$ is $n$, $\mathbf{A}$ is an $n$ by $n$ matrix, $c$ is a scalar, and row vector $\mathbf{x}^T$ is the

TABLE II
PSEUDOCODE OF DIRECT PHYSICS-BASED MOR PROCESS

***Input***: inductance matrix $M$, potance matrix $pp$ of an initial PEEC circuit.

***Output***: Inductance $M$, potance matrix $pp$ of a new simplified PEEC circuit.

1. Initial $X=0$ and set MOR criterion $\delta$.
2. Find node $k$ with minimum $\left|\omega_{\max}^2(M_{ik,ik}^k+2X_{k,ik}^k)/Npp_{k,k}^k\right|$.
3. **while** $\left|\omega_{\max}^2(M_{ik,ik}^k+2X_{k,ik}^k)/Npp_{k,k}^k\right|<\delta$
4. Reassign terminal notations according to node $k$.
5. General Y-Δ transformation with low-pass approximation.

$$pp_{i,j}^k = Npp_{k,k}^k,\ pp_{i,j}^k = 0,\ M_{i(i+1),j(j+1)}^k = M_{ik,jk}^k - M_{ik,(j+1)k}^k - M_{(i+1)k,jk}^k + M_{(i+1)k,(j+1)k}^k$$
$$pp_{i,s}^k = pp_{k,s}^k,\ X_{i,mn}^k = M_{ik,mn}^k + X_{k,mn}^k,\ X_{s,i(i+1)}^k = X_{s,ik}^k - X_{s,(i+1)k}^k$$
$$M_{i(i+1),mn}^k = M_{ik,mn}^k - M_{(i+1)k,mn}^k,\ X_{i,j(j+1)}^k = M_{ik,jk}^k + X_{k,jk}^k - M_{ik,(j+1)k}^k - X_{k,(j+1)k}^k$$

6. Combine parallel potors and parallel inductors according to Table I.
7. Reassign node number for transformed circuit.
8. Find node $k$ with minimum $\left|\omega_{\max}^2(M_{ik,ik}^k+2X_{k,ik}^k)/Npp_{k,k}^k\right|$
9. **End while**
10. Convert mixed couplings into inductive couplings.

transpose of vector **x**. With a conventional vector-by-vector-transpose multiplication scheme, the computational overhead on the outer product for absorbing one node is on the order of $O(n^2)$. Therefore, the total computational overhead of the outer product for an MOR process is on the order of $O(N^3)$.

From the above discussion, it can be concluded that the computational overhead is dominated by the outer products in the combining processes, which takes more than 95% of overall computing time according to many numerical case studies. The good news is that the outer product calculation can be significantly accelerated by multicore parallel computation using a massive GPU acceleration technology.

## IV. NUMERICAL EXAMPLES

The proposed direct mesh-based MOR method can compress the original PEEC circuit with lumped elements into a concise circuit in the same circuit configuration. Examples 1 and 2 will demonstrate that the resultant circuits have a clear physical meaning. For a large-scale high-speed circuit, the MOR method can reduce the order of the original circuit by more than an order of magnitude. Consequently, the computing time for circuit domain simulation can be reduced by more than three orders of magnitude as shown by example 3, in which both conductor and dielectric losses are taken into account.

### A. Example 1

The first example is a spiral inductor printed on a substrate with $\varepsilon_r = 4$ as depicted in Fig. 8. The inner radius $R$ is 62 $\mu$m, the trace width $W_m$ is 10 $\mu$m, and the trace spacing $W_s$ is 3 $\mu$m. The thickness of the substrate is 3 $\mu$m and the height of the conductor bridge is also 3 $\mu$m. The conductor is treated as an infinitely thin perfect conductor.

The meshing scheme of the structure for PEEC modeling is superimposed in Fig. 8. The original PEEC model of this

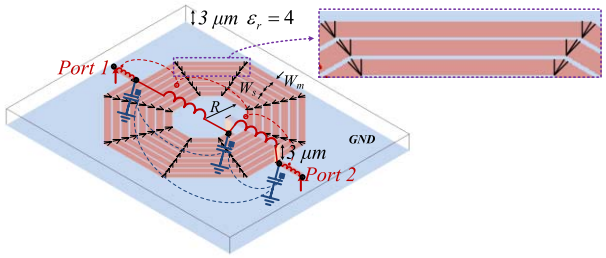


Fig. 8. Spiral inductor layout of example 1 and its order-reduced circuit.

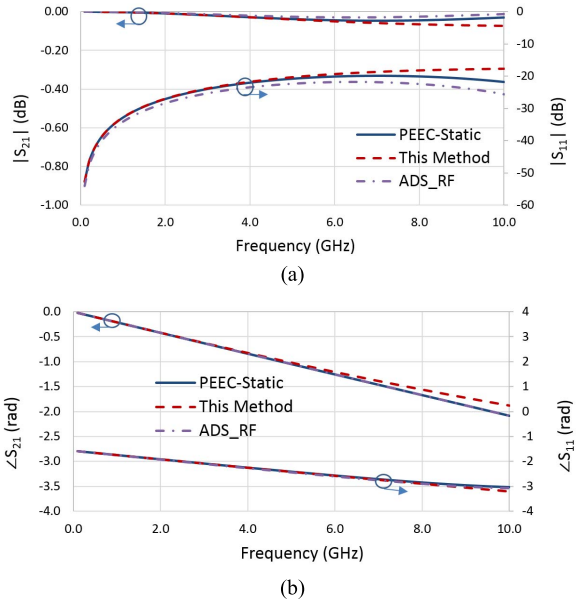


Fig. 9. Computed S-parameters by the PEEC model, this method, and ADS. (a) Magnitude of S-parameters. (b) Phase of S-parameters.

RF inductor contains 190 nodes, 188 capacitors coupled with each other, and 189 inductors coupled with each other.

This PEEC model is reduced to a concise circuit as depicted in Fig. 8 in less than a second. With the low-pass criterion set to 0.2 and cutoff frequency set to 10 GHz, the model-order reduced circuit is with five nodes, three capacitors coupled with each other, and four inductors coupled with each other.

S-parameters obtained from the PEEC model, this method, and the commercial softwave ADS (RF momentum module) are given in Fig. 9. As can be observed, both the magnitude and phase of the S-parameters by the three methods agree well in the frequency range of 0–10 GHz.

### B. Example 2

The second example is a multilayer bandpass filter as depicted in Fig. 10. This filter consists of three metal layers in the substrate with a dielectric constant of 7.8. The height of each layer is 91.44 $\mu$m. The other dimensions of this circuit are marked in Fig. 10. In this case, the conductor is treated as an infinitely thin perfect conductor. To create a quasi-static PEEC circuit model of this layered media circuit problem, the full-wave Green's functions at 1 MHz are used for calculating the capacitors and inductors.

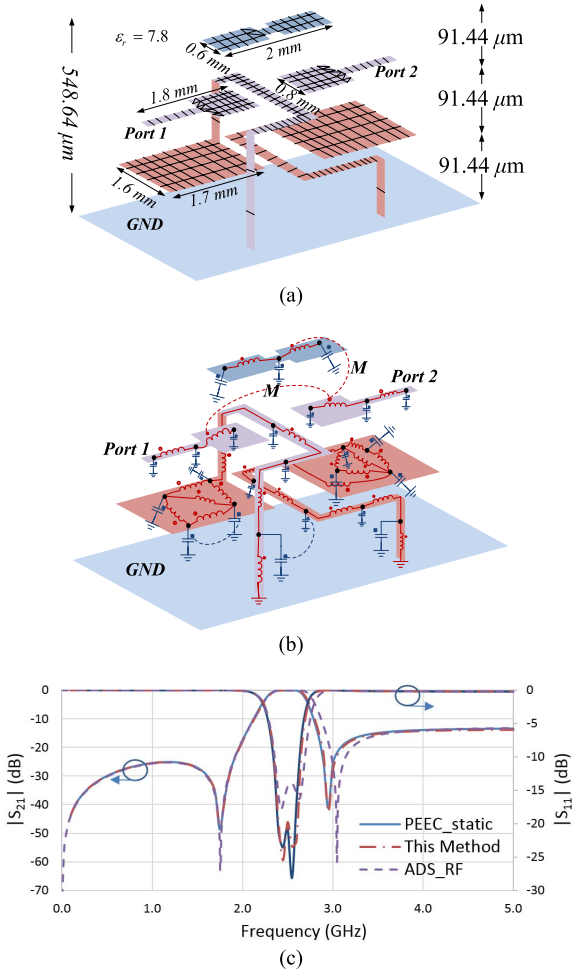


Fig. 10. Example of an LTCC bandpass filter. (a) LTCC bandpass filter layout. (b) Lumped circuit after MOR by this method. (c) Computed S-parameters of the PEEC, this method, and ADS.

The meshing scheme of this structure for the PEEC modeling is shown in Fig. 10. The original PEEC model consists of 243 nodes, 243 potors coupled with the rest of the potors, and 363 inductors coupled with the rest of the inductors.

With the low-pass criterion as 0.02 and the cutoff frequency set to 5 GHz, the PEEC model is reduced to the concise circuit model shown in Fig. 10(b) in 5 s. The reduced circuit consists of 26 nodes, 26 potors coupled with each other, and 29 inductors coupled with every inductor.

The S-parameters of the bandpass filter by PEEC model, this method, and those from RF momentum module of ADS are given in Fig. 10(c). Good agreement, especially between those by the PEEC model and this method, can be observed.

It would be interesting to investigate the system poles of the $Y$ matrix of circuit change during the MOR process. The $Y$ matrix is defined to describe port voltage–current relation obtained from system matrices related to all nodes' voltages and elements' currents [10]. Table III lists the system poles from the most significant pole (with the smallest value) to the least significant pole (with the largest value). The poles correspond to the imaginary part of the eigenvalues of the $Y$ matrix, whose values are the angular eigenfrequencies of the system. Since the full-wave Green's functions at a very low frequency are used, a very small real part of each pole exists but is ommitted in the table. It is found, from Table III, that the significant system poles are retained nearly unchanged in the MOR process. During each recursive process, absorbing the most insignificant node that satisfies the low-pass criterion most is equivalent to redistributing the contribution of the least important pole to the second or third least important poles.

TABLE III
SYSTEM POLES OF $Y$ MATRIX DURING MOR PROCESS

| Pole Index | Circuit Size | 243 nodes 363 inductors | 28 nodes 32 inductors | 27 nodes 31 inductors | 26 nodes 29 inductors |
|---|---|---|---|---|---|
| 1 | ($\times 10^{10}$) | 1.3943 | 1.4006 | 1.4008 | 1.4018 |
| 2 | ($\times 10^{10}$) | 1.6066 | 1.6138 | 1.6142 | 1.6148 |
| 3 | ($\times 10^{10}$) | 5.0825 | 5.3787 | 5.3820 | 5.3817 |
| … | … | … | … | … | … |
| 26 | ($\times 10^{6}$) | $3.8172\times10^{5}$ | 1.4930 | 1.6373 | 7.6536 |
| 27 | ($\times 10^{6}$) | $3.8661\times10^{5}$ | 8.3455 | 8.5753 | |
| 28 | ($\times 10^{6}$) | $3.9444\times10^{5}$ | 3.6558 | | |
| … | … | … | | | |
| 243 | ($\times 10^{12}$) | 2.9153 | | | |

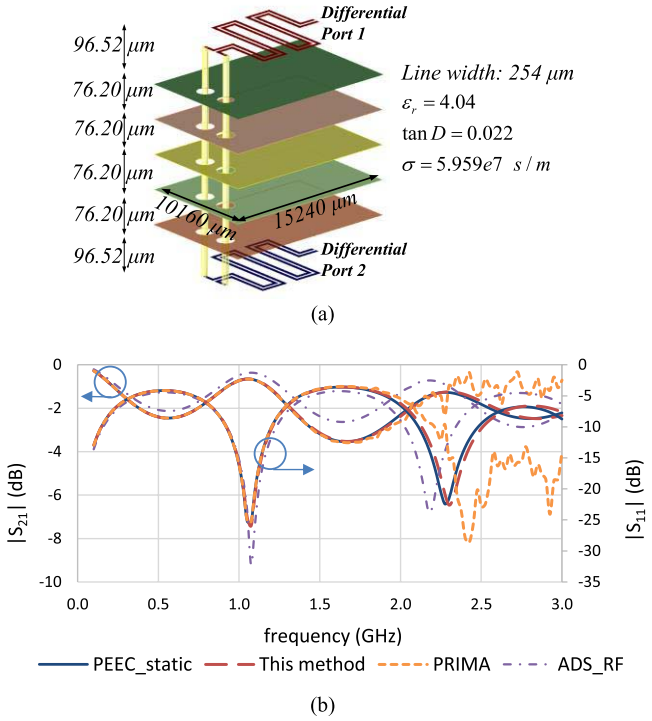


Fig. 11. Multilayer through via circuit with a differential signal line. (a) Circuit layout of the through via problem. (b) Computed S-parameters by the PEEC model, this method, PRIMA, and ADS.

## C. Example 3

The last example is a typical multilayer interconnection circuit with through via holes and a differential signal line. The circuit's overall size is 10 160 $\mu$m × 15 240 $\mu$m × 497.84 $\mu$m as shown in Fig. 11(a). There are five layers of power plates and two layers of signal traces which are connected by a pair of vias in the substrate with a dielectric constant of 4.04 and loss tangent of 0.022. In the PEEC model, the metal thickness is set

TABLE IV
CIRCUIT SIZE AND COMPUTATION TIME OF PEEC MODEL AND THIS METHOD

| | PEEC model | This method |
|---|---|---|
| No. of nodes | 4,012 | 379 |
| No. of potors | 4,098 | 377 |
| No. of capacitive couplings | 8,394,753 | 70,876 |
| No. of inductors | 7,061 | 715 |
| No. of inductive couplings | 24,925,330 | 255,255 |
| Preprocessing time | 0 sec | 0 sec |
| MOR time | N/A | 83 min 4 sec |
| S-parameters simulation time | 410 min 22 sec | 17 sec |
| Total time | 410 min 22 sec | 83 min 21 sec |

TABLE V
COMPUTATION OF PRIMA MODEL AND THIS METHOD

| | PRIMA model | This method |
|---|---|---|
| Model order | 1,094 | 1,094 (379 nodes +715 ind.+2 ports) |
| Preprocessing time | 13 min 54 sec | 0 sec |
| Time of MOR process | 137 min 20 sec | 83 min 4sec |
| S-parameter simulation time | 20 sec | 17 sec |
| Total time | 151 min 34 sec | 83 min 21sec |
| Average relative error of $\|s_{11}\|$ | 32.33% | 1.6324% |
| Maximum relative error of $\|s_{11}\|$ | 214.8% | 6.0471% |
| Average relative error of $\|s_{21}\|$ | 15.17% | 1.0034% |
| Maximum relative error of $\|s_{21}\|$ | 86.67% | 3.4951% |

to 12 $\mu$m and its conductivity is set to $5.959 \times 10^7$ S $\cdot$ m$^{-1}$. The other dimensions are shown in Fig. 11(a). The values of full-wave Green's functions at 100 MHz are used in this example.

In the original PEEC model, all the metal surfaces, including via holes, are meshed by triangular and rectangular meshes (not shown). In the PEEC model, there is a mutual capacitive coupling between every pair of potors and mutual inductive coupling between every pair of inductors. Although all the conductor losses are frequency dependent in principle, in this example, only the conductor loss at a high frequency of $f = 3$ GHz is used in the original PEEC model.

As shown in Table IV, with the low-pass criterion set to 0.008 and cutoff frequency set to 3 GHz, the order of the original PEEC model can be reduced by about one order of magnitude and the S-parameter simulation time can be reduced by three orders of magnitude.

Besides, this example is also analyzed by the PRIMA model [10], a Krylov-based MOR technique. The preprocessing time, MOR computing time, circuit simulation time, and the average and maximum relative errors of S-parameters of this method and the Krylov-based technique are compared in Table V. The major attributes of the two models are summarized as follows.

1) This proposed method directly uses the coefficients of potential matrix and the inductance matrix of the PEEC model, but the PRIMA method needs to use the inductance matrix and the capacitance matrix which are obtained by inverting large coefficients of potential matrix.
2) The computed S-parameters by the PEEC model, this method, the PRIMA model, and ADS momentum RF module are compared in Fig. 11(b). It is seen that the S-parameters by the PRIMA method do not converge to those of the PEEC model in the high-frequency range. This is because the vectors of Krylov subspace quickly converge to an eigenvector corresponding to a dominant eigenvalue of the moment matrix. This issue was also stated in [16].
3) For lossless problems, the Krylov-based PRIMA technique suffers from the inversion of an ill-conditioned MNA matrix. By introducing an artificial loss, the order-reduced model is no longer lossless [9].
4) The order of the order-reduced model by this method is automatically determined subject to the user-specified low-pass criterion. But the order for a PRIMA model is determined by trial and error.
5) The order-reduced PRIMA model is a full matrix so that there is no clear correspondence between the macromodel and a circuit model.

It is clearly shown through this example that the proposed method is effective for a large-scale circuit problem with superior convergence, better accuracy, and faster computing time than those of the PRIMA model.

For this example, all the algorithms of the PEEC model, the PRIMA model, and this proposed method are executed by Fortran programs using one thread serially. The CPU of this computer is Intel Core i7-3770 CPU at 3.4 GHz.

## V. CONCLUSION

This paper presents a brand new MOR method for analyzing a large-scale high-speed/microwave circuit. The method starts with the traditional PEEC model. By introducing a general circuit transformation that can be directly applied to the circuit configuration of the PEEC model, the proposed MOR method progressively reduces the order of the original problem by at least one order of magnitude without involving any matrix operations. This feature warrants that the method will not suffer from the scalability problem as long as the storage space is sufficient. Another attractive feature of this method is that its computational overhead is dominated by the operation of outer products in combining processes, which takes more than 95% of overall computing time. This feature allows the MOR process to be significantly accelerated by multicore parallel computation using a massive GPU acceleration technology. In addition to its computational advantage, the proposed method also provides a physically meaningful lumped circuit model. Three practical examples are given to demonstrate the effectiveness and the accuracy of the new method compared with the PRIMA model, a traditional mathematics-based MOR model. It has been shown that the proposed method is capable of not only significantly reducing the order of a large-scale circuit but also retaining its physical insight of the original circuit.

## APPENDIX I
## GENERAL Y-$\Delta$ CIRCUIT TRANSFORMATION

In the node-absorbing process, a circuit model consists of not only capacitive couplings between potors and inductive

couplings between inductors but also mixed couplings between potors and inductors. A general Y-$\Delta$ circuit transformation for absorbing one node in such a circuit is derived in detail in this appendix.

### A. Updating Elements Associated With New Potors

Applying linear superposition principle and KVL equation (12a), the voltage across $pp_{i,i}^k$ in the transformed circuit can be written in terms of the original circuit shown in Fig. 5 as

$$\begin{aligned} V_{i0}^k = &\sum_{j=1}^{N} j\omega M_{ik,jk}^k I_{jk}^k + j\omega X_{k,ik}^k I_{k0}^k + \sum_{(m,n)} j\omega M_{ik,mn}^k I_{mn} \\ &+ \sum_s j\omega X_{s,ik}^k I_{s0} + \frac{pp_{k,k}^k}{j\omega} I_{k0}^k + \sum_{j=1}^{N} j\omega X_{k,jk}^k I_{jk}^k \\ &+ \sum_{(m,n)} j\omega X_{k,mn}^k I_{mn} + \sum_s \frac{pp_{k,s}^k}{j\omega} I_{s0}. \end{aligned} \tag{A-1}$$

With KCL equation (13), the voltage can be expressed as

$$\begin{aligned} V_{i0}^k = &\left[\frac{Npp_{k,k}^k}{j\omega} + j\omega\left(M_{ik,ik}^k + 2X_{k,ik}^k\right)\right] I_{i0}^k \\ &+ \sum_{(m,n)} j\omega\left(M_{ik,mn}^k + X_{k,mn}^k\right) I_{mn} \\ &+ \sum_{j=1, j\neq i}^{N} j\omega\left(M_{ik,jk}^k + X_{k,ik}^k + X_{k,jk}^k\right) I_{j0}^k \\ &+ \sum_s \left(\frac{pp_{k,s}^k}{j\omega} + j\omega X_{s,ik}^k\right) I_{s0} \\ &+ \sum_{j=1}^{N} j\omega\left(M_{ik,jk}^k + X_{k,jk}^k - M_{ik,(j+1)k}^k - X_{k,(j+1)k}^k\right) \\ &\times I_{j(j+1)}^k. \end{aligned} \tag{A-2}$$

From (A-2), the transformed circuit elements related to the newly added potor $pp_{i,i}^k$ can be updated by

$$\begin{aligned} pp_{i,i}^k &= Npp_{k,k}^k - \omega^2\left(M_{ik,ik}^k + 2X_{k,ik}^k\right) \\ pp_{i,j}^k &= -\omega^2\left(M_{ik,jk}^k + X_{k,ik}^k + X_{k,jk}^k\right) \\ X_{i,j(j+1)}^k &= M_{ik,jk}^k + X_{k,jk}^k - M_{ik,(j+1)k}^k - X_{k,(j+1)k}^k \\ pp_{i,s}^k &= pp_{k,s}^k - \omega^2 X_{s,ik}^k, \quad X_{i,mn}^k = M_{ik,mn}^k + X_{k,mn}^k \end{aligned} \tag{A-3}$$

which are, respectively, the self-potance, capacitive couplings between newly added potors, mixed couplings between newly added potors and newly introduced inductors, capacitive couplings between newly added potors and the remaining potors, and mixed couplings between newly added potors and the remaining inductors.

### B. Updating Elements Associated With New Inductors

Applying the linear superposition principle and KVL equation (12b), the voltage across inductor $M_{i(i+1),i(i+1)}^k$ can be obtained by

$$\begin{aligned} V_{i(i+1)}^k &= V_{ik}^k - V_{(i+1)k}^k \\ &= j\omega X_{k,ik}^k I_{k0}^k + \sum_{j=1}^{N} j\omega M_{ik,jk}^k I_{jk}^k \\ &\quad + \sum_s j\omega X_{s,ik}^k I_{s0} - j\omega X_{k,(i+1)k}^k I_{k0}^k \\ &\quad - \sum_{j=1}^{N} j\omega M_{(i+1)k,jk}^k I_{jk}^k - \sum_{(m,n)} j\omega M_{(i+1)k,mn}^k I_{mn} \\ &\quad - \sum_s j\omega X_{s,(i+1)k}^k I_{s0}. \end{aligned} \tag{A-4}$$

With KCL equation (13), the voltage can be expressed as

$$\begin{aligned} V_{i(i+1)}^k = &\sum_{j=1}^{N} j\omega\left(M_{ik,jk}^k - M_{ik,(j+1)k}^k - M_{(i+1)k,jk}^k \right. \\ &\left. + M_{(i+1)k,(j+1)k}^k\right) I_{j(j+1)}^k \\ &+ \sum_{j=1}^{N} j\omega\left(M_{ik,jk}^k + X_{k,ik}^k - M_{(i+1)k,jk}^k - X_{k,(i+1)k}^k\right) I_{j0}^k \\ &+ \sum_{(m,n)} j\omega\left(M_{ik,mn}^k - M_{(i+1)k,mn}^k\right) I_{mn} \\ &+ \sum_s j\omega\left(X_{s,ik}^k - X_{s,(i+1)k}^k\right) I_{s0}. \end{aligned} \tag{A-5}$$

From (A-5), the transformed circuit elements related to the newly introduced inductor $M_{i(i+1),i(i+1)}^k$ can be updated by

$$\begin{aligned} M_{i(i+1),j(j+1)}^k &= M_{ik,jk}^k - M_{ik,(j+1)k}^k - M_{(i+1)k,jk}^k \\ &\quad + M_{(i+1)k,(j+1)k}^k \\ X_{j,i(i+1)}^k &= M_{ik,jk}^k + X_{k,ik}^k - M_{(i+1)k,jk}^k - X_{k,(i+1)k}^k \\ M_{i(i+1),mn}^k &= M_{ik,mn}^k - M_{(i+1)k,mn}^k \\ X_{s,i(i+1)}^k &= X_{s,ik}^k - X_{s,(i+1)k}^k \end{aligned} \tag{A-6}$$

which are, respectively, inductive couplings (including self-inductance) between newly introduced inductors, mixed couplings between newly added potors and newly introduced inductors, inductive couplings between newly introduced inductors and the remaining inductors, and mixed couplings between the remaining potors and newly introduced potors.

### C. Updating Elements Associated With Remaining Potors

Applying the linear superposition principle, the voltage across $pp_{s,s}^k$ can be obtained by

$$\begin{aligned} V_{s0}^k = &\frac{pp_{s,k}^k}{j\omega} I_{k0}^k + \sum_{i=1}^{N} j\omega X_{s,ik}^k I_{ik}^k + \sum_{(m,n)} j\omega X_{s,mn} I_{mn} \\ &+ \sum_t \frac{pp_{s,t}}{j\omega} I_{t0}. \end{aligned} \tag{A-7}$$

With KCL equation (13), the voltage can be expressed as

$$V_{s0}^k = \sum_{i=1}^{N}\left(\frac{pp_{s,k}^k}{j\omega} + j\omega X_{s,ik}^k\right) I_{i0}^k + \sum_{i=1}^{N} j\omega (X_{s,ik}^k - X_{s,(i+1)k}^k) I_{i(i+1)}^k + \sum_t \frac{pp_{s,t}}{j\omega} I_{t0} + \sum_{(m,n)} j\omega X_{s,mn} I_{mn}. \quad \text{(A-8)}$$

It can be found from (A-8) that the transformed circuit elements related to potor $pp_{s,s}^k$ can be updated as

$$pp_{s,i}^k = pp_{s,k}^k - \omega^2 X_{s,ik}^k, \quad X_{s,i(i+1)}^k = X_{s,ik}^k - X_{s,(i+1)k}^k$$
$$pp_{s,t} = pp_{s,t}, \quad X_{s,mn} = X_{s,mn} \quad \text{(A-9)}$$

which are, respectively, capacitive couplings between remaining potors and newly added potors, mixed couplings between remaining potors and newly introduced inductors, capacitive couplings between remaining potors, and mixed couplings between remaining potors and inductors.

### D. Updating Elements Associated With Remaining Inductors

Applying the linear superposition principle, the voltage across the remaining inductor $M_{mn,mn}^k$ can be obtained by

$$V_{mn}^k = j\omega X_{k,mn}^k I_{k0}^k + \sum_{i=1}^{N} j\omega M_{mn,ik}^k I_{ik}^k + \sum_{(s,t)} j\omega M_{mn,st} I_{st} + \sum_s j\omega X_{s,mn} I_{s0}. \quad \text{(A-10)}$$

With KCL equation (12), the voltage can be expressed by

$$V_{mn}^k = \sum_{i=1}^{N} j\omega\left(M_{mn,ik}^k - M_{mn,(i+1)k}^k\right) I_{i(i+1)}^k + \sum_{i=1}^{N} j\omega\left(M_{mn,ik}^k + X_{k,mn}^k\right) I_{i0}^k + \sum_{(s,t)} j\omega M_{mn,st} I_{st} + \sum_s j\omega X_{s,mn} I_{s0}. \quad \text{(A-11)}$$

From (A-11), the transformed circuit elements related to the remaining inductor $M_{mn,mn}^k$ can be updated as

$$M_{mn,i(i+1)}^k = M_{mn,ik}^k - M_{mn,(i+1)k}^k$$
$$X_{i,mn}^k = M_{mn,ik}^k + X_{k,mn}^k$$
$$M_{mn,st} = M_{mn,st}, \quad X_{s,mn} = X_{s,mn} \quad \text{(A-12)}$$

which are, respectively, inductive couplings between remaining inductors and newly introduced inductors, mixed couplings between newly added potors and remaining inductors, inductive couplings between remaining inductors, and mixed couplings between remaining potors and inductors.

## APPENDIX II
## COMBINING TWO COUPLED SHUNT ELEMENTS

Using (34) and (35) in (39) yields

$$\begin{aligned} V_{mn} &= Z_{ij,mn}^a I_{ij}^a + Z_{ij,mn}^a I_{ij}^a + \sum_{(s,t)} Z_{mn,st} I_{st} \\ &= \left\{ I_{ij}/Y_t + \sum_{(s,t)} \left[\left(Y_{ij}^a + Y_{ij}^{ab}\right) Z_{ij,st}^a + \left(Y_{ij}^b + Y_{ij}^{ab}\right) Z_{ij,st}^b\right] \times I_{st}/Y_t \right\} \times \left[\left(Y_{ij}^a + Y_{ij}^{ab}\right) Z_{ij,mn}^a + \left(Y_{ij}^b + Y_{ij}^{ab}\right) Z_{ij,mn}^b\right] \\ &\quad + \sum_{(s,t)} Z_{mn,st} I_{st} - \sum_{(s,t)} \left(Y_{ij}^a Z_{ij,st}^a Z_{ij,mn}^a + Y_{ij}^{ab} Z_{ij,st}^a Z_{ij,mn}^b \right. \\ &\quad \left. + Y_{ij}^{ab} Z_{ij,st}^b Z_{ij,mn}^a + Y_{ij}^b Z_{ij,st}^b Z_{ij,mn}^b\right) I_{st} \\ &= \left[\left(Y_{ij}^a + Y_{ij}^{ab}\right) Z_{ij,mn}^a + \left(Y_{ij}^b + Y_{ij}^{ab}\right) Z_{ij,mn}^b\right] I_{ij}/Y_t \\ &\quad + \sum_{(s,t)} Z_{mn,st} I_{st} \\ &\quad + \sum_{(s,t)} \left\{ \left[\left(Y_{ij}^{ab}\right)^2 - Y_{ij}^a Y_{ij}^b\right] Z_{ij,st}^a Z_{ij,mn}^a \right. \\ &\qquad + \left[Y_{ij}^a Y_{ij}^b - \left(Y_{ij}^{ab}\right)^2\right] Z_{ij,st}^a Z_{ij,mn}^b \\ &\qquad + \left[Y_{ij}^a Y_{ij}^b - \left(Y_{ij}^{ab}\right)^2\right] Z_{ij,st}^b Z_{ij,mn}^a \\ &\qquad \left. + \left[\left(Y_{ij}^{ab}\right)^2 - Y_{ij}^a Y_{ij}^b\right] Z_{ij,st}^b Z_{ij,mn}^b \right\} I_{st}/Y_t \\ &= \left[\left(Y_{ij}^a + Y_{ij}^{ab}\right) Z_{ij,mn}^a + \left(Y_{ij}^b + Y_{ij}^{ab}\right) Z_{ij,mn}^b\right] I_{ij}/Y_t \\ &\quad + \sum_{(s,t)} \left[Z_{mn,st} - \left(\left(Y_{ij}^{ab}\right)^2 - Y_{ij}^a Y_{ij}^b\right)\left(Z_{ij,mn}^a - Z_{ij,mn}^b\right) \right. \\ &\qquad \left. \times \left(Z_{ij,st}^a - Z_{ij,st}^b\right)\right] I_{st}/Y_t. \end{aligned} \quad \text{(A-13)}$$

## REFERENCES


[1] A. E. Ruehli, "Equivalent circuit models for three-dimensional multiconductor systems," *IEEE Trans. Microw. Theory Techn.*, vol. MTT-22, no. 3, pp. 216–221, Mar. 1974.

[2] V. Vahrenholt, H.-D. Brüns, and H. Singer, "Fast EMC analysis of systems consisting of PCBs and metallic antenna structures by a hybridization of PEEC and MoM," *IEEE Trans. Electromagn. Compat.*, vol. 52, no. 4, pp. 962–973, Nov. 2010.

[3] A. E. Ruehli and A. C. Cangellaris, "Progress in the methodologies for the electrical modeling of interconnects and electronic packages," *Proc. IEEE*, vol. 89, no. 5, pp. 740–771, May 2001.

[4] L. K. Yeung and K.-L. Wu, "Generalized partial element equivalent circuit (PEEC) modeling with radiation effect," *IEEE Trans. Microw. Theory Techn.*, vol. 59, no. 10, pp. 2377–2384, Oct. 2011.

[5] L. K. Yeung and K.-L. Wu, "PEEC modeling of radiation problems for microstrip structures," *IEEE Trans. Antennas Propag.*, vol. 61, no. 7, pp. 3648–3655, Jul. 2013.

[6] D. Daroui and J. Ekman, "PEEC-based simulations using iterative method and regularization technique for power electronic applications," *IEEE Trans. Electromagn. Compat.*, vol. 56, no. 6, pp. 1448–1456, Dec. 2014.

[7] J. Wang and K.-L. Wu, "A derived physically expressive circuit model for multilayer RF embedded passives," *IEEE Trans. Microw. Theory Techn.*, vol. 54, no. 5, pp. 1961–1968, May 2006.

[8] H. Hu, K. Yang, K.-L. Wu, and W.-Y. Yin, "Quasi-static derived physically expressive circuit model for lossy integrated RF passives," *IEEE Trans. Microw. Theory Techn.*, vol. 56, no. 8, pp. 1954–1961, Aug. 2008.

[9] P. Feldmann and R. W. Freund, "Efficient linear circuit analysis by Padé approximation via the Lanczos process," *IEEE Trans. Comput.-Aided Design Integr.*, vol. 14, no. 5, pp. 639–649, May 1995.

[10] A. Odabasioglu, M. Celik, and L. T. Pileggi, "PRIMA: Passive reduced-order interconnect macromodeling algorithm," *IEEE Trans. Comput.-Aided Design Integr. Circuits Syst.*, vol. 17, no. 8, pp. 645–654, Aug. 1998.
[11] F. Ferranti, M. S. Nakhla, G. Antonini, T. Dhaene, L. Knockaert, and A. E. Ruehli, "Multipoint full-wave model order reduction for delayed PEEC models with large delays," *IEEE Trans. Electromagn. Compat.*, vol. 53, no. 4, pp. 959–967, Nov. 2011.
[12] F. Ferranti, G. Antonini, T. Dhaene, L. Knockaert, and A. E. Ruehli, "Physics-based passivity-preserving parameterized model order reduction for PEEC circuit analysis," *IEEE Trans. Compon., Packag. Manuf. Technol.*, vol. 1, no. 3, pp. 399–409, Mar. 2011.
[13] F. Ferranti, G. Antonini, T. Dhaene, and L. Knockaert, "Guaranteed passive parameterized model order reduction of the partial element equivalent circuit (PEEC) method," *IEEE Trans. Electromagn. Compat.*, vol. 52, no. 4, pp. 974–984, Nov. 2010.
[14] Y. Dou, L. K. Yeung, and K.-L. Wu, "An matrix inversion-less derived physically expressive circuit model for quasi-static multiple conductor EM problems," in *Proc. IEEE Int. Conf. NEMO*, Ottawa, ON, Canada, Aug. 2015, pp. 1–3.
[15] D. K. Cheng, "Static electric fields," in *Field and Wave Electromagnetics*, 2nd ed. Reading, MA, USA: Addison-Wesley, 1989, pp. 129–131.
[16] R. W. Freund, "Model reduction methods based on Krylov subspaces," *Acta Numer.*, vol. 12, pp. 267–319, May 2013.

**Yuhang Dou** (S'13) received the B.S. degree in electronics engineering from the Nanjing University of Science and Technology, Nanjing, China, in 2012. She is currently pursuing the Ph.D. degree at The Chinese University of Hong Kong, Hong Kong.

Her current research interests include partial element equivalent circuit (PEEC) modeling, full-wave circuit domain modeling for signal integrity and electromagnetic compatibility problems, and physics-based model order reduction of PEEC model for electromagnetic problems in both the frequency and time domains.

Ms. Dou was the recipient of Honorable Mention of the 2015 IEEE MTT-S Conference on Numerical Electromagnetic and Multiphysics Modeling and Optimization Student Paper Competition She was the first runner-up (MTT section) of the 2015 IEEE (HK) Section AP/MTT Postgraduate Conference Student Paper Competition.

**Ke-Li Wu** (M'90–SM'96–F'11) received the B.S. and M.Eng. degrees from the Nanjing University of Science and Technology, Nanjing, China, in 1982 and 1985, respectively, and the Ph.D. degree from Laval University, Quebec, QC, Canada, in 1989.

He was with the Communications Research Laboratory, McMaster University, Hamilton, ON, Canada, as a Research Engineer and a Group Manager from 1989 to 1993. In 1993, he joined the Corporate R&D Division, COM DEV International Ltd., Cambridge, ON, Canada, the largest Canadian space equipment manufacturer, where he was a Principal Member of the Technical Staff. Since 1999, he has been with The Chinese University of Hong Kong, Hong Kong, where he is currently a Professor and the Director of the Radiofrequency Radiation Research Laboratory. He has authored or co-authored numerous publications in the areas of EM modeling and microwave passive components, microwave filter, and antenna engineering. His current research interests include partial element equivalent circuit and derived physically expressive circuit EM modeling of high speed circuits, RF and microwave passive circuits and systems, synthesis theory and practices of microwave filters, antennas for wireless terminals, LTCC-based multichip modules, and RF identification technologies.

Prof. Wu is a Member of the IEEE MTT-8 Subcommittee (Filters and Passive Components) and serves as a TPC Member for many prestigious international conferences, including the IEEE MTT-S International Microwave Symposium. He was a recipient of the 1998 COM DEV Achievement Award and the Asia–Pacific Microwave Conference Prize in 2008 and 2012, respectively. He was an Associate Editor of the IEEE TRANSACTIONS ON MICROWAVE THEORY AND TECHNIQUES from 2006 to 2009.